PROCEEDINGS OF SCIENCE

Multimessenger astronomy driven by high-energy neutrinos

Shigeru Yoshida[a,*]

[a] *International Center for Hadron Astrophysics, Chiba University, Chiba 263-8522, Japan*

E-mail: syoshida@hepburn.s.chiba-u.ac.jp

The possible connection between high energy neutrinos in the energy region above 100 TeV and ultrahigh energy cosmic rays (UHECRs) at energies above 10^{19} eV motivates multi-messenger observation approaches involving neutrinos and the multi-wavelength electro-magnetic (EMG) signals. We have constructed a generic unification scheme to model the neutrino and UHECR common sources. Finding the allowed space of the parameters on the source characteristics allows a case study to evaluate the likelihood of each of the known source classes being such unified sources. The likely source candidates are transient or flaring objects mainly in optical and X-ray bands. We propose the two feasible strategies to identify these sources. One is to introduce a sub-threshold triggering in a wide field of view X-ray observatory for following up neutrino detections, and the other is to search for EMG counterparts associated with detections of multiple neutrino events coming from the same direction within a time scale of $\lesssim 30$ days. Sources with a total neutrino emission energy greater than $\sim 10^{51}$ erg are accessible with the present or near-future high energy neutrino observation facilities collaborating with X-rays and optical telescopes currently in operation. The neutrino-driven multi-messenger observations provide a smoking gun to probe the hadronic emission sources we would not be able to find otherwise.

38th International Cosmic Ray Conference (ICRC2023)
26 July - 3 August, 2023
Nagoya, Japan

*Speaker

© Copyright owned by the author(s) under the terms of the Creative Commons Attribution-NonCommercial-NoDerivatives 4.0 International License (CC BY-NC-ND 4.0).

PoS(ICRC2023)015

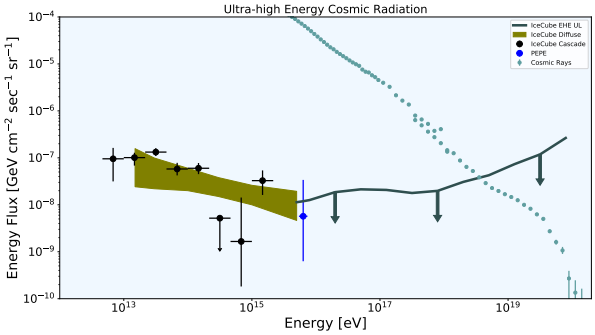

Figure 1: The energy fluxes of UHE cosmic background radiations. The small data points represent the UHECR fluxes measured by PAO [1]. The rest of the data shows the neutrino energy fluxes and the upper limits measured with IceCube. The thick black data points were obtained by the neutrino-induced cascade measurements [4]. The shaded region indicates the flux space consistent with the ν_μ induced track measurements [5]. The blue data point shows the flux of the 6 PeV-energy $\bar{\nu}_e$ event estimated by the dedicated search channel (PEPE) [6]. The thick line with arrows indicates the differential upper limit obtained by the Extremely-high Energy (EHE) neutrino search [7]. The neutrino fluxes are the all-flavor-sum fluxes $E_\nu^2\Phi_{\nu_e+\nu_\mu+\nu_\tau}$.

1. Introduction

The cosmic background radiation in ultra-high energy (UHE) sky at $\gg$ TeV is formed by cosmic rays and neutrinos. The precise measurements of ultrahigh-energy cosmic rays (UHECRs) by Pierre Auger Observatory (PAO) with high statistics have now revealed the detailed structure of their energy spectrum [1]. The IceCube Neutrino Observatory has discovered [2, 3] and measured the high energy neutrino radiation in the UHE sky [4, 5], realizing the observation window of the penetrating messengers to study the UHE emissions. As shown in Fig. 1, we have found that the observed energy flux of high-energy neutrinos above $\sim$ 100 TeV is comparable to that of UHECRs at $\gtrsim 10^{19}$ eV. It suggests that the neutrino radiation may originate in the same astronomical objects to radiate UHECRs we have been detecting. It may be plausible that the UHE cosmic radiation can be understood in a common unified scheme.

We have built the unification generic model to account for the observed neutrinos at energies greater than $\sim$ 100 TeV and UHECRs, based on the photo-hadronic interaction framework [8]. This modeling enables us to evaluate if a given class of astronomical objects are qualified as the possible common origin of UHECRs and neutrinos. It is a viable tool to probe the UHECR origin with the multi-messenger observations.

In this article, we discuss the possibilities of the UHECR-neutrino common sources for a broad spectrum of the astronomical objects classes with the generic unification model. We then discuss how we can identify these sources. As the viable source candidates are transients, we argue that neutrino follow-up observations in optical and X-ray bands are feasible methods to find the sources of hadronic emissions. We propose practical strategies to pin down neutrino sources that could not be identified by neutrino observations alone.

PoS(ICRC2023)015

Finally, we conclude that multi-messenger observations with neutrinos, optical, and X-ray photons pioneer in the field of high energy astrophysics with the presently and soon-to-be available facilities.

2. A generic unification model

We constructed the generic framework to describe a unified origin of UHECRs and high energy neutrinos with the parameterization less dependent on the details of the source environment and the model-dependent micro-physics processes [8]. Our goal here is to derive generic and model-independent constraints on characteristics of the possible UHECR-neutrino common emitters. The resultant constraints are considered to be conservative and weaker than those obtained by the model-dependent arguments applied to each of the specific classes of astronomical objects, but the results based on our generic framework are universal and robust as long as the UHE particle emission mechanism is mostly determined in a simple setup with physics processes well approximated by a first leading order effect. We introduce the Occam's razor principle here to judge whether a given astronomical object class can be the unified origin. In this sense, our arguments provide a guidance for astronomers to conduct the multi-messenger observations.

We made the following assumptions to build our generic unification framework.

One zone

The cosmic ray accelerations and their interactions to produce secondary neutrinos occur in the same place.

Escape from sources

The energy spectrum of accelerated UHECRs running away from the acceleration zone is not drastically distorted in their escape process. This assumption may affect the UHECR energetics condition we will discuss below. Considering the uncertainties of the UHECR escape process, we use the measured UHECR intensity as the upper limit to constrain the source luminosity rather than to fit it with the spectrum calculated by the generic model.

Optically thin environment

The sources are optically thin for UHE protons interacting with photons, and their emission is directly observed without absorption. This assumption is valid for photo-hadronic scenarios with one zone modelling.

Photon spectrum

The spectrum of photons interacting with UHECRs to produce neutrinos is described by a power-law. However we note that the thermal photon yield can also be reasonably approximated by a power-law form in the energy range relevant to the high energy neutrino emission within a factor of two allowance.

Cosmological evolution

The UHECR-neutrino common sources follow the cosmological evolution tracing the

PoS(ICRC2023)015

star formation rate (SFR) or any other similar evolutions. However, we parameterize the evolutions to estimate the conditions for the different evolution cases when necessary.

2.1 The source modelling

The power of the unified sources is gauged by the bolometric photon luminosity

$$L'_\gamma = 4\pi R^2 c \int_{\varepsilon_\gamma^{\rm min}}^{\varepsilon_\gamma^{\rm max}} \frac{dn_\gamma}{d\varepsilon'_\gamma} \varepsilon'_\gamma d\varepsilon'_\gamma, \tag{1}$$

where R is the distance of the UHECR acceleration and emission site from the source center. Primed (') characters represent quantities measured in the rest frame of plasma with the Lorentz bulk factor Γ. The photon density spectrum follows a power-law form as

$$\frac{dn_\gamma}{d\varepsilon'_\gamma} = \frac{K'_\gamma}{\varepsilon'_{\gamma 0}} \left(\frac{\varepsilon'_\gamma}{\varepsilon'_{\gamma 0}} \right)^{-\alpha_\gamma}, \tag{2}$$

where $\varepsilon'_{\gamma 0}$ is the reference energy in the engine frame, and it is associated with the representative energy of UHECRs ε_{p0}^Δ by

$$\varepsilon_{\gamma 0} = \frac{(s_R - m_p^2)}{4} \frac{\Gamma^2}{\varepsilon_{p0}^\Delta} \tag{3}$$

where $s_R \approx 1.47$ GeV^2 is the Mandelstam variable at the Δ resonance in the photopion production. The representative CR energy ε_{p0}^Δ is set to be 10 PeV in the present formulation, as this energy range of cosmic ray protons should produce the PeV-energy neutrinos IceCube has detected. The spectrum of UHECRs emitted from the sources is assumed to follow a power-law with index of $\alpha_{\rm CR}$.

The bolometric luminosity of UHECRs at energies above $\varepsilon_{p0}^\Delta = 10$ PeV is connected to L_γ via the CR loading factor $\xi_{\rm CR}$ as $L_{\rm CR} \approx \xi_{\rm CR} L_\gamma = \xi_{\rm CR} L'_\gamma \Gamma^2$.

The neutrino luminosity with respect to a given $L_{\rm CR}$ is determined by the $p\gamma$ interaction optical depth, an average number of the interaction times before cosmic ray protons escape from the interaction site. It is approximately given by [8]

$$\begin{aligned}
\tau_{p\gamma}(\varepsilon_i) &\approx \tau_{p\gamma 0} \left(\frac{\varepsilon_i}{\tilde{\varepsilon}_{p0}^\Delta} \right)^{\alpha_\gamma - 1} \\
&\approx \left[\frac{2}{1+\alpha_\gamma} \frac{K'_\gamma R}{\Gamma} \int ds \frac{\sigma_{p\gamma}(s)}{s - m_p^2} \right] \left(\frac{\varepsilon_i}{\tilde{\varepsilon}_{p0}^\Delta} \right)^{\alpha_\gamma - 1} \qquad (4) \\
&\approx \frac{B'}{\Gamma^2} \sqrt{\frac{L'_\gamma}{\xi_B}} C(\alpha_\gamma, \tilde{\varepsilon}_{p0}^\Delta) \left(\frac{\varepsilon_i}{\tilde{\varepsilon}_{p0}^\Delta} \right)^{\alpha_\gamma - 1}. \qquad (5)
\end{aligned}$$

Proceeding from Eq. (4) to (5), the explicit dependence on R is eliminated by considering the energy density balance between the photon radiation L'_γ and the magnetic energy with

PoS(ICRC2023)015

the B-field strength B' via the equipartition parameter ξ_B. The constant C depends only on the photon spectrum power-law index α_γ and the representative CR energy $\varepsilon_{p0}^{\Delta}$ and is approximately given by

$$\begin{aligned} C(\alpha_\gamma, \tilde{\varepsilon}_{p0}^{\Delta}) &\sim 2.4 \times 10^{-24}\ \mathrm{erg}^{-1}\ \mathrm{cm}^{3/2}\ \mathrm{s}^{1/2} \\ &\times \left(\frac{2}{1+\alpha_\gamma}\right)\left(\frac{\tilde{\varepsilon}_{p0}^{\Delta}}{10\ \mathrm{PeV}}\right). \end{aligned} \tag{6}$$

2.2 The required source conditions

A UHECR source must meet the following necessity conditions : The acceleration, the escape, and the survival requirements.

In order to accelerate cosmic rays to UHE range, the acceleration time must be faster than the dynamical time scale. It sets the lower bound for the magnetic field as

$$B' \gtrsim \frac{\varepsilon_i^{\max}}{eZ}\frac{\eta}{R} \approx 1.1 \times 10^5 \eta \left(\frac{R}{3\times 10^{12}\ \mathrm{cm}}\right)^{-1}\left(\frac{\varepsilon_i^{\max}}{Z 10^{11}\ \mathrm{GeV}}\right)\ \mathrm{G}, \tag{7}$$

where $\eta \gtrsim 1$ is the particle acceleration efficiency term. This condition, also known as the Hillas condition when $\eta \to \beta^{-2}$, can be transformed to the constraint on the target photon luminosity L'_γ, the gauge of the source engine power in the present generic modelling scheme,

$$L'_\gamma \geq \frac{1}{2}\xi_B^{-1} c \eta^2 \beta^2 \left(\frac{\varepsilon_i^{\max}}{Ze}\right)^2 \tag{8}$$

$$\simeq 1.7 \times 10^{45}\ \xi_B^{-1}\eta^2\beta^2\left(\frac{\varepsilon_i^{\max}}{Z 10^{11}\ \mathrm{GeV}}\right)^2\ \mathrm{erg/s} \tag{9}$$

In addition, to ensure that UHECRs can leave the sources before losing their energies, the escape time scale must be faster than the cosmic ray energy loss time scale. The energy loss processes consist of the $p\gamma$ photo-meson production, Bethe-Heitler (BH) interactions, and the synchrotron cooling. The photo-meson production time scale is essentially counted with the $p\gamma$ optical depth, $\tau_{p\gamma}$, in the present scheme, and any sources with $\tau_{p\gamma}(\varepsilon_i^{\max}) \lesssim 1$ implies that the energy loss by the $p\gamma$ photo-meson production is not a deciding factor to limit the UHECR acceleration and escape processes. We examine this $\tau_{p\gamma}$ condition by estimating $\tau_{p\gamma}$ using Eq. (5) in Section 2.4. As the BH process is in general important only if the photon spectrum is softer as $\alpha_\gamma \gtrsim 2$, the UHECR escape condition is formulated as a necessity condition by requiring the dynamical time scale faster than the synchrotron cooling time scale. It has been found that this condition is transformed to the upper bound of the $p\gamma$ optical depth at the cosmic ray reference energy $\varepsilon_{p0}^{\Delta} = 10$ PeV, $\tau_{p\gamma 0}$, as

$$\tau_{p\gamma 0} \lesssim 6 \times 10^{-1}\frac{2}{1+\alpha_\gamma}\left(\frac{\xi_B}{0.1}\right)^{-1}\left(\frac{A}{Z}\right)^4\left(\frac{\varepsilon_i^{\max}}{10^{11}\ \mathrm{GeV}}\right)^{-1}. \tag{10}$$

If the measured bulk of UHECRs is dominated by heavier nuclear rather than nucleon as strongly indicated by the data obtained by PAO, the further severe requirement must

PoS(ICRC2023)015

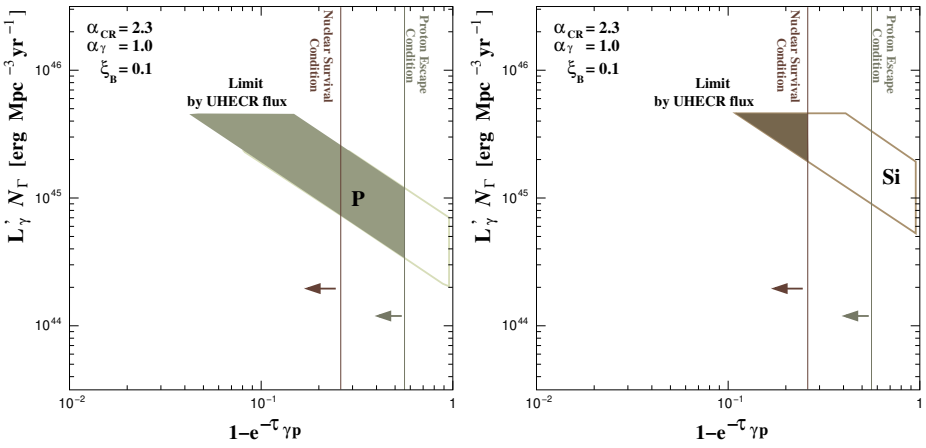

Figure 2: The allowed region in the parameter space of luminosity per unit volume, $L'_\gamma \mathcal{N}_\Gamma$, and damping factor $1 - e^{-\tau_{p\gamma 0}}$ [8]. The region enclosed by the solid lines displays the allowed space by the UHECR and the neutrino flux requirements. The shaded region represents the parameter space allowed also by considering the UHECR proton escape condition or the nuclear survival condition. The left panel shows the proton model while the right panel shows the case of primary silicon nuclei.

be satisfied – The nuclei survival condition [9]. That is, we require that nuclei with $A > 1$ and $Z > 1$ are accelerated and survive. This is possible only if the time scale of the photo-disintegration is slower than the dynamical time scale which leads to the condition on photo-disintegration optical depth as $\tau_{A\gamma} \lesssim A$. We found that this condition sets the upper bound of the $p\gamma$ optical depth as [8]

$$\begin{aligned} \tau_{p\gamma 0} &\lesssim A \frac{\int ds \frac{\sigma_{p\gamma}(s)}{s-m_p^2}}{\int ds \frac{\sigma_{A\gamma}(s)}{s-m_A^2}} \left[\left(\frac{s_{\rm GDR} - m_A^2}{s_R - m_p^2} \right) \left(\frac{\tilde{\varepsilon}^\Delta_{p0}}{\varepsilon_i^{\rm max}} \right) \right]^{\alpha_\gamma - 1} \\ &\lesssim 0.4 \left(\frac{A}{56} \right)^{0.79} = 0.2 \left(\frac{A}{24} \right)^{0.79} . \end{aligned} \tag{11}$$

2.3 The constraints due to the UHECR and and neutrino fluxes

UHECR sources in the unification scenario must provide both the UHECR flux and the high energy neutrino flux that are consistent with the measurements. The analytical formulation to calculate the spectrum of UHECRs on the Earth and that of secondary produced neutrinos have been derived in Ref. [8, 10] to place the constraints on the source parameters of L'_γ, $\tau_{p\gamma 0}$, and the boosted source number density $N_\Gamma \equiv n_0 \xi_{\rm CR} \Gamma^2$ where n_0 is the comoving number density in the present epoch. Note that $L'_\gamma N_\Gamma = \xi_{\rm CR} L_\gamma n_0 = L_{\rm CR} n_0$ is the bolometric luminosity density of UHECRs above $\varepsilon^\Delta_{p0} = 10$ PeV. Figure 2 shows the resultant constraints. The region enclosed in the solid lines is the allowed parameter space by the flux conditions. The conditions were set by the criteria that ensure the consistency to the neutrino measurements with IceCube including the upper limit of flux at $\varepsilon_\nu \gtrsim 100$ PeV, and that the UHECR flux on the earth would not exceed the integral flux above 10^{19} eV measured by PAO.

PoS(ICRC2023)015

We can interpret the allowed parameter space shown in Fig. 2 from the context of the UHECR energetics and the analytical estimate of the fiducial neutrino flux. The UHECR differential luminosity density is estimated as [11]

$$E_{\rm CR}\frac{dQ_{\rm CR}}{dE_{\rm CR}} \approx 6.3\times10^{43}[{\rm erg\ Mpc^{-3}yr^{-1}}]\left(\frac{E_{\rm CR}}{10^{19.5}\ {\rm eV}}\right)^{2-\alpha_{\rm CR}} \approx \begin{cases} 1.8\times10^{44}\ [{\rm erg\ Mpc^{-3}yr^{-1}}] & \alpha_{\rm CR}=2.3, E_{\rm CR}=10^{18}\ {\rm eV} \\ 3.4\times10^{44}\ [{\rm erg\ Mpc^{-3}yr^{-1}}] & \alpha_{\rm CR}=2.5, E_{\rm CR}=10^{18}\ {\rm eV} \end{cases} \quad (12)$$

As a representative case, we consider $\alpha_{\rm CR}=2.3$ hereafter. From Eq. (12), the resultant bolometric UHECR energy density above the reference energy above $\varepsilon_{p0}^{\Delta}=10$ PeV is given by

$$n_0\xi_{\rm CR}L_\gamma \approx 13E_{\rm CR}\frac{dQ_{\rm CR}}{dE_{\rm CR}}|_{E_{\rm CR}=10^{18}\ {\rm eV}} \approx 2.3\times10^{45}\ \ {\rm erg\ Mpc^{-3}yr^{-1}}, \quad (13)$$

which is consistent with the allowed region of the parameter space. This energetics condition above effectively sets the requirement of the CR loading factor for a given L_Γ and n_0 such as

$$\xi_{\rm CR}\approx0.7\left(\frac{L_\gamma}{10^{46}{\rm erg/s}}\right)^{-1}\left(\frac{n_0}{10^{-8}{\rm Mpc^{-3}}}\right)^{-1}. \quad (14)$$

The neutrino emissivity from a source is connected to the primary UHECR emissivity as [12]

$$\varepsilon_\nu^2\frac{d\dot{N}_\nu}{d\varepsilon_\nu}\approx\xi_\pi<x><y_\nu>\tau_{p\gamma}\varepsilon_{\rm CR}^2\frac{d\dot{N}_{\rm CR}}{d\varepsilon_{\rm CR}}A^{2-\alpha_{\rm CR}} \quad (15)$$

for a hadronically thin (*i.e.*$\tau_{p\gamma}\lesssim5$) source. Here $\xi_\pi\sim3/2$ is the average multiplicity of neutrinos from a single pion produced by the photo-hadronic interaction, and $<y_\nu>\sim1/4$ is the average fraction of energy channeling into a neutrino from the secondary produced pion and $<x>\sim0.2$ is the average ineasticity of the $p\gamma$ collision. Since the energy flux of the high energy cosmic background neutrinos can be approximately written using the source emissivity $\varepsilon_\nu^2 d\dot{N}_\nu/d\varepsilon_\nu$, we can relate the $p\gamma$ optical depth to the required bolometric UHECR luminosity density for a given energy flux of neutrinos via Eq. (15). We get

$$\tau_{p\gamma0}L'_\gamma\mathcal{N}_\Gamma=\tau_{p\gamma0}n_0\xi_{\rm CR}L_\gamma \approx 9.3\times10^{43}\left(\frac{E_\nu^2\Phi_\nu}{2\times10^{-8}\ [{\rm GeV\ cm^{-2}\ sec^{-1}sr^{-1}}]}\right) \times\left(\frac{\xi_z}{2.8}\right)^{-1}A^{0.3}\ \ {\rm erg\ Mpc^{-3}yr^{-1}}, \quad (16)$$

for $\alpha_{\rm CR}=2.3$. Here $\xi_z\equiv(1/t_{\rm H})\int dt\Psi(z)/(1+z)$ is a dimensionless parameter that depends on the redshift evolution function $\Psi(z)$ of the sources. This relation well represents the allowed parameter space shown in Fig. 2.

PoS(ICRC2023)015

	AGN corona	BL Lac	FSRQ	Radio Gal. MAD
Γ of the target photons	≈ 1	≈ 10	≈ 1	≈ 1
target photon energy: Eq. (3)	opt/UV/X-ray	X-ray	UV/Opt	UV/Opt
L_γ [erg/s]	10^{44}	2×10^{44}	4×10^{46}	10^{41}
n_0 [Mpc^{-3}]	5×10^{-6}	3×10^{-7}	3×10^{-10}	2×10^{-6}
B' [G]	300	1	1	100
$\xi_{\rm B}$	13	75	0.1	4×10^5
Acceleration: Eq. (9)	$\xi_{\rm B}\gtrsim 0.087(\frac{Z}{14})^{-2}$	$\xi_{\rm B}\gtrsim 4.3(\frac{Z}{14})^{-2}$	$\xi_{\rm B}\gtrsim 0.04(\frac{Z}{1})^{-2}$	$\xi_{\rm B}\gtrsim 87(\frac{Z}{14})^{-2}$
$\tau_{p\gamma0}$ by Escape: Eq. (10)	$\lesssim 0.005(\frac{\xi_B}{13})^{-1}$	$\lesssim 7.5\times10^{-4}(\frac{\xi_B}{80})^{-1}$	$\lesssim 0.6(\frac{\xi_B}{0.1})^{-1}$	$\lesssim 8\times10^{-8}(\frac{\xi_B}{4\times10^5})^{-1}$
$\tau_{p\gamma0}$ by Nuclei survival: Eq. (11)	$\lesssim 0.2(\frac{A}{28})^{0.79}$	$\lesssim 0.2(\frac{A}{28})^{0.79}$	$\lesssim 0.2(\frac{A}{28})^{0.79}$	$\lesssim 0.2(\frac{A}{28})^{0.79}$
$\tau_{p\gamma0}$ by ν Flux: Eq. (17)	$\gtrsim 0.1(\frac{\xi_z}{2.8})^{-1}(\frac{A}{28})^{0.3}$	$\gtrsim 0.1(\frac{\xi_z}{2.8})^{-1}(\frac{A}{28})^{0.3}$	$\gtrsim 0.01(\frac{\xi_z}{8.4})^{-1}$	$\gtrsim 0.5(\frac{\xi_z}{0.6})^{-1}(\frac{A}{28})^{0.3}$
$\xi_{\rm CR}$: Eq. (14)	≈ 1.2	≈ 1.2	≈ 5.8	≈ 350

Table 1: The parameters of the neutrino emission characteristics in the unification model and the constraints on ξ_B, the B-field equipartition parameter, and $\tau_{p\gamma0}$, the photo-hadronic optical depth at the cosmic ray reference energy of $\varepsilon_{p0}^{\Delta}=10$ PeV imposed by the conditions for UHECR-neutrino common sources. The various sites/population in AGN family are listed.

Combining the UHECR luminosity density given by Eq. (13) with this neutrino fiducial flux condition, Eq. (16), sets the lower bound of the $p\gamma$ optical depth, which is

$$\begin{aligned}\tau_{p\gamma0} &\gtrsim 0.04A^{0.3}\left(\frac{\xi_z}{2.8}\right)^{-1}\\ &\gtrsim 0.1\left(\frac{A}{28}\right)^{0.3}\left(\frac{\xi_z}{2.8}\right)^{-1}.\end{aligned}\tag{17}$$

As the UHECR escape condition sets the *upper* bound of the optical depth (see Eq. (10)), this fiducial neutrino flux requirements leads to a necessity condition of the B-field equipartition parameter.

$$\xi_{\rm B}\lesssim 1.5\left(\frac{A}{Z}\right)^4\left(\frac{\xi_z}{2.8}\right)\left(\frac{\varepsilon_i^{\rm max}}{10^{11}\ {\rm GeV}}\right)^{-1}A^{-0.3}\tag{18}$$

2.4 The case study

Tables 1 and 2 list the various source classes together with their characteristic parameters and the constraints on ξ_B and $\tau_{p\gamma0}$ imposed by the conditions we discussed earlier.

The AGN corona [13] is already disfavored as a common UHECR neutrino source regardless of any model-dependent arguments. The conditions on $\tau_{p\gamma}$ from the UHECR escape and the fiducial neutrino flux requirements cannot hold concurrently. This is primarily because the corona is expected to be strongly magnetized ($\xi_{\rm B}\gg1$). The approximate estimate using Eq. (5) gives $\tau_{p\gamma}\approx 100\left(B'/0.3{\rm kG}\right)\left(L_\gamma/10^{44}{\rm erg/s}\right)^{\frac{1}{2}}\left(\xi_B/13\right)^{-\frac{1}{2}}\left(\beta/0.02\right)^{-1}\left(\varepsilon_i/\tilde{\varepsilon}_{p0}^{\Delta}\right)^{0.8}$, indicating that AGN corona may be a TeV-PeV neutrino source candidate, but certainly not a UHECR source since $\tau_{p\gamma}\gg1$ prevents hadrons from being accelerated to UHE range.

The BL Lac [14] should also meet the contradicting $\tau_{p\gamma}$ conditions demanded by the UHECR escape and neutrino fiducial flux requirements, which makes it difficult to be considered as a common source. The estimated optical depth is $\tau_{p\gamma0}\approx 4\times10^{-6}\left(B'/1{\rm G}\right)\left(\Gamma/10\right)^{-3}\left(L_\gamma/2\times10^{44}{\rm erg/s}\right)^{\frac{1}{2}}\left(\xi_B/80\right)^{-\frac{1}{2}}$, which indeed suggests that BL Lacs may be UHECR sources but too dark in neutrinos.

UHE emission from FSRQ [15] is an interesting possibility. The UHECR escape and the neutrino flux conditions can be concurrent in principle, providing that $\tau_{p\gamma0}\sim$

PoS(ICRC2023)015

	jetted TDE	TDE corona	Low Luminosity GRB	Engine-driven SNe afterglow
Γ of the target photons	≈ 10	≈ 1	≈ 2–10	≈ 1
target photon energy: Eq. (3)	X-ray	opt/UV/X-ray	X-ray	UV/Opt
L_γ [erg/s]	10^{47}	3×10^{43}	10^{47}	3×10^{45}
n_0 [Mpc^{-3}]	$3\times10^{-12}(\frac{\Delta T}{10^6\mathrm{s}})$	$4\times10^{-7}(\frac{\Delta T}{10^7\mathrm{s}})$	$3\times10^{-11}(\frac{\Delta T}{3\times10^3\mathrm{s}})$	$10^{-9}(\frac{\Delta T}{10^4\mathrm{s}})$
B' [G]	500	10^3	80	1.6
ξ_B	1	45	0.1	4
Acceleration: Eq. (9)	$\xi_\mathrm{B}\gtrsim 0.009(\frac{Z}{14})^{-2}$	$\xi_\mathrm{B}\gtrsim 0.3(\frac{Z}{14})^{-2}$	$\xi_\mathrm{B}\gtrsim 0.009(\frac{Z}{14})^{-2}$	$\xi_\mathrm{B}\gtrsim 0.3(\frac{Z}{14})^{-2}$
$\tau_{p\gamma0}$ by Escape: Eq. (10)	$\lesssim 0.06(\frac{\xi_\mathrm{B}}{1})^{-1}$	$\lesssim 1.3\times10^{-3}(\frac{\xi_B}{45})^{-1}$	$\lesssim 0.6(\frac{\xi_B}{0.1})^{-1}$	$\lesssim 0.015(\frac{\xi_B}{4})^{-1}$
$\tau_{p\gamma0}$ by Nuclei survival: Eq. (11)	$\lesssim 0.2(\frac{A}{28})^{0.79}$	$\lesssim 0.2(\frac{A}{28})^{0.79}$	$\lesssim 0.2(\frac{A}{28})^{0.79}$	$\lesssim 0.2(\frac{A}{4})^{0.79}$
$\tau_{p\gamma0}$ by ν Flux: Eq. (17)	$\gtrsim 0.5(\frac{\xi_z}{0.5})^{-1}(\frac{A}{28})^{0.3}$	$\gtrsim 0.5(\frac{\xi_z}{0.5})^{-1}(\frac{A}{28})^{0.3}$	$\gtrsim 0.1(\frac{\xi_z}{2.8})^{-1}(\frac{A}{28})^{0.3}$	$\gtrsim 0.1(\frac{\xi_z}{2.8})^{-1}(\frac{A}{28})^{0.3}$
ξ_CR: Eq. (14)	≈ 220	≈ 5.6	≈ 24	≈ 24

Table 2: Same as Table 1 but the various transient objects are listed.

$0.1-1$ is in the plausible range at the FSRQ system. Using Eq. (5), we indeed estimate $\tau_{p\gamma}\approx 1.4\left(B'/1\mathrm{G}\right)\left(L_\gamma/4\times10^{46}\mathrm{erg/s}\right)^{\frac{1}{2}}\left(\xi_B/0.1\right)^{-\frac{1}{2}}\left(\varepsilon_i/\tilde{\varepsilon}^{\Delta}_{p0}\right)^{0.5}$. The high photon luminosity ($L_\gamma\gtrsim10^{46}$ erg/s) meets the acceleration condition given by Eq. (9) for protons ($Z=1$) even if $\xi_\mathrm{B}\ll1$ while the nuclei survival condition could be only barely satisfied. It implies that FSRQs may be the common origin for UHECR protons and neutrinos, though not UHECR nuclei. However, this hypothesis is disfavored, since the strongly evolved sources such as FSRQs are not likely to be UHECR origins if the proton component is not negligible at the UHE range [16, 17]. This is because the GZK cosmogenic neutrinos would have overshot the present upper limit of neutrino flux at EeV (10^{18} eV) range placed by IceCube and PAO.

A scenario of hadronic emissions from magnetically arrested disks (MAD) in a subclass of radio galaxies has been proposed [18], motivated by the GeV-TeV gamma-ray observations from nearby radio galaxies. The cosmic ray accelerations can be plausible with the framework of radiatively inefficient accretion flows (RIAFs). Because of the highly magnetized environment ($\xi_\mathrm{B}\gg100$), MAD may be producing UHECR nuclei though UHECR protons cannot escape. It certainly meets the acceleration condition given by Eq. (9) for silicons ($Z=14$). The energetics condition, Eq. (14), requires $\xi_\mathrm{CR}\gg10$ but this constraints can be relaxed if we expand this model to the entire Fanaroff-Riley I galaxies by including high-excitation radio galaxies, bringing $n_0\approx10^{-4}$ Mpc^{-3}. However, it is unlikely to emit neutrinos with the intensity measured by IceCube. The approximate estimate using Eq. (5) gives $\tau_{p\gamma}\approx2.5\times10^{-3}\left(B'/100\mathrm{G}\right)\Gamma^{-3}\left(L_\gamma/10^{41}\mathrm{erg/s}\right)^{\frac{1}{2}}\left(\xi_B/3.7\times10^5\right)^{-\frac{1}{2}}\left(\varepsilon_i/\tilde{\varepsilon}^{\Delta}_{p0}\right)^{1.2}$, which is far below the fiducial neutrino flux condition, Eq. (17). This is primarily because the MAD is optically too thin, given that the luminosity of the target photons (optical/UV) $L_\gamma\sim10^{41}$ erg/s. Note that the high magnetic field strength would cause the synchrotron cooling of the secondary produced muons by the photo-hadronic collisions, which suppresses neutrinos with energies higher than ~10 PeV.

Powerful transient objects (table 2) have also been discussed in the literature for considering UHECR origins. Jetted TDEs cannot be UHECR proton sources because of the escape requirement, but potentially UHE nuclei sources [19]. However, the tight margin between the nuclei survival condition and the fiducial neutrino flux requirement needs a fine parameter tuning for qualifying this object to be the UHECR-neutrino common sources. The ap-

PoS(ICRC2023)015

proximate estimate indeed gives $\tau_{p\gamma} \approx 0.34 \left(B'/500\mathrm{G}\right) (\Gamma/10)^{-3} \left(L_\gamma/10^{47}\mathrm{erg/s}\right)^{\frac{1}{2}} \xi_B^{-\frac{1}{2}} \left(\varepsilon_i/\tilde{\varepsilon}_{p0}^{\Delta}\right)$ which could barely meet the both conditions, considering the unavoidable uncertainties of the parameter values. The more serious issue is that it is more difficult to meet the energetics condition. The resultant CR loading factor $\xi_{\rm CR} \gg 10$ raises questions about credibility of the TDE scenario.

Non-jetted TDEs are more generous objects and may alleviate the energetics issue. The wind driven by TDE or the possible corona may be a plausible site for cosmic-ray acceleration [20]. The demerit is their possible optically thick environment. The TDE corona scenario expects $\tau_{p\gamma} \approx 20 \left(B'/1\mathrm{kG}\right) \Gamma^{-3} \left(L_\gamma/3\times10^{43}\mathrm{erg/s}\right)^{\frac{1}{2}} (\xi_B/45)^{-\frac{1}{2}} (\beta/0.1)^{-1} \left(\varepsilon_i/\tilde{\varepsilon}_{p0}^{\Delta}\right)^{0.8}$ and the UHE nuclei cannot survive. The high magnetic field ($\sim$ kG) naturally sets such dense photon environment that break down nuclei via photo-disintegration. UHECR protons cannot escape either.

Low Luminosity GRBs [21] are among the most promising candidates for the unification scenario. The estimated optical depth, $\tau_{p\gamma} \approx 0.1 \left(B'/80\mathrm{G}\right) (\Gamma/10)^{-3} \left(L_\gamma/10^{47}\mathrm{erg/s}\right)^{\frac{1}{2}} (\xi_B/0.1)^{-\frac{1}{2}} \left(\varepsilon_i/\tilde{\varepsilon}_{p0}^{\Delta}\right)^{1.2}$ exactly meets all the conditions as listed in table 2. The CR lading factor required for the UHECR energetics may be high, but it can be relaxed, given that the rate density $\rho_0 \sim 3\times10^{-7}$ Mpc^{-3}yr^{-1} is still quite uncertain.

The external acceleration during the afterglow of engine-driven SNe has also been among the UHECR nuclei emission models [22]. As seen in Table 2, the UHECR escape condition prevents the afterglow from being the common UHECR protons and neutrino sources regardless of model-dependent arguments. Just as in the other transients, there is the (tight) margin to meet both the nuclei survival condition and the fiducial neutrino flux requirement. However, the estimate using Eq. (5) gives $\tau_{p\gamma} \approx 1.1\times10^{-4} \left(B'/1.6\mathrm{G}\right) (\Gamma/10)^{-3} \left(L_\gamma/3\times10^{45}\mathrm{erg/s}\right)^{\frac{1}{2}} (\xi_B/4)^{-\frac{1}{2}} \left(\varepsilon_i/\tilde{\varepsilon}_{p0}^{\Delta}\right)^{0.7}$, which does not satisfy the neutrino flux condition. This source is hadronically too thin to explain the 100 TeV-PeV energy neutrinos measured by IceCube.

3. Identification of UHECR sources with neutrino follow-up observations

Many of the potential high energy neutrino/UHECR sources are transient emitters. Low Luminosity GRBs, or jetted-TDEs are among the representative examples. SNe with strong interaction with circumstellar material and other non-relativistic transients may contribute to the TeV neutrino sky [23, 24] although they are unlikely to be the sources of UHECRs. Moreover, the neutrino emissions from jets in AGNs (e.g., FSRQs) are expected to occur in flare rather than a steady manner [25]. Thus it is a powerful method to search for electromagnetic (EMG) counterparts by follow-up observations triggered by a neutrino detection in order to identify neutrino or UHECR sources.

It is straightforward to find the neutrino-EMG association with a rare type of the objects. The GeV-energy gamma-ray blazars detected by Fermi-LAT belong to this category. However more abundant classes of objects such as SNe or low-luminosity GRBs would yield more frequent chance coincidences between neutrino and EMG detections, which makes it

PoS(ICRC2023)015

challenging to claim robust associations. Moreover, the optical sky is filled with many SNe irrelevant from neutrino emissions (e.g., type Ia) and they cause significant contamination in optical follow-ups. The longer duration of neutrino transient emissions reaching to weeks expected from circumstellar SNe or TDEs would yield even more severe contamination by the unrelated SNe. The simple multi-messenger strategy faces the difficulty here.

There are two feasible solutions. The first approach is to conduct follow-up observations in X-ray band. The X-ray sky is quieter as SNe are not luminous X-ray transients. The drawback is that many of the neutrino source candidates we discussed above may not be bright enough for the existing X-ray telescopes with the rapid follow-up capability. The low luminosity GRBs are good examples. Their dim luminosity of $L_{\rm X} \sim 10^{47}$ erg/s is below the regular detection threshold unless a progenitor happens to be located in the neighborhood of our galaxy. It is, therefore, necessary to implement a sub-threshold detection trigger on a X-ray observatory with wide field of view. The Monitor of All-sky X-ray Image (MAXI) telescope [26] can meet this demand as it is regularly monitoring all sky at a single photon counting level. The MAXI-IceCube coincidence search with the sub-threshold detection algorithms will be scheduled in near future.

The second approach is to search for neutrino multiplet, two (doublet) or more neutrinos originating from the same direction within a certain time frame [27]. Since only nearby sources can yield detectable neutrino multiplets, we can rule out any distant EMG transient counterpart candidates found in a follow-up observation triggered by a multiplet detection. Therefore, searches for the neutrino-optical association can be performed under less contaminated environment. It has been found that ~ 90 % of sources to produce detectable neutrino multiplets by a 1 km^3 neutrino telescope are localized within $z \lesssim 0.15$ while the distribution of sources to yield a singlet neutrino detection extends up to $z \gtrsim 2$ [27]. Confining neutrino sources within the local universe realizes the following strategy of optical follow-up observations for claiming robust neutrino-optical associations.

We anticipate $\gtrsim 100$ SNe in an optical follow-up observation to search for any optical counterpart. They are mostly not associated with the neutrino detection as mentioned earlier, though it is always possible that one of them can be the real counterpart. Using the fact that sources producing neutrino multiplet are localized in the low redshift universe, we can distinguish unassociated SNe from the source to emit neutrino multiplet. Among the optical transients found in a follow-up observation triggered by a neutrino multiplet detection, the closest object is the most likely neutrino source. Because the expected redshift distribution of the source to yield neutrino doublet is quite different from that of unassociated SNe, we can judge if the closest counterpart is indeed associated with the neutrino doublet detection in a statistical way. Figure 3 shows the probability distributions of the redshift of the closest object for the two possibilities. The pronounced difference between them can construct a test statistic to examine which hypothesis is favored. For example, finding an SN-like transient at $z = 0.04$ (≈ 170 Mpc) in an optical follow-up observation leads to $\sim 2.7\sigma$ significance against the hypothesis of the incorrect coincident SN detection.

Identifying the closest object from the numerous transients found in an optical survey triggered by the neutrino detection requires extensive spectroscopic measurements, which

PoS(ICRC2023)015

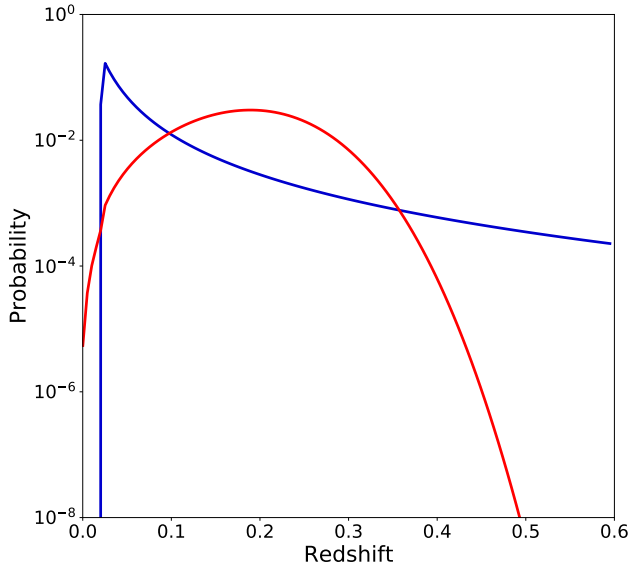

Figure 3: Probability distribution of the redshift of the closest counterpart with bin size $\Delta z = 0.005$ [27]. The bin size is chosen for illustrative purposes. The blue curve represents the case of the signal hypothesis that the object is the neutrino source to yield the detected neutrino multiplet, and the red curve shows the case of the coincident background hypothesis, that is the chance coincident detection of an unassociated SN. $\mathcal{E}_\nu^{\rm fl} = 1 \times 10^{49}$ erg and $R_0 = 3 \times 10^{-6}$ Mpc^{-3} yr^{-1} are assumed for the multiplet source.

may not always be feasible. One of the practical solutions is to rely on the photometric redshift of the host galaxies whose information is available in the data taken by the survey facilities with the wide field of view such as the Vera C. Rubin Observatory. Another way to perform the intensive spectroscopy will be brought by the prime focus spectrograph on Subaru [28]. It has a remarkable capability of a wide-field simultaneous spectrography with high multiplicity. It is of great importance for neutrino and optical astronomers to closely collaborate for discoveries of yet unknown transient neutrino sources.

Searches for neutrino multiplets are powerful not just for reliably identifying the EMG counterparts, but also for revealing/constraining the source characteristics. Figure 4 shows the number of sources to yield detectable neutrino multiples, $N_{\Delta\Omega}^{\rm M}$, from the sky patch of $\Delta\Omega = 1$ deg^2 [27]. The search time scale is assumed to be $\Delta T = 30$ days, considering the typical time scale of the neutrino transient emission from TDEs and core-collapse SNe and being long enough to cover faster transients such as low luminosity GRBs and GRB afterglow. Only the diagonal region is displayed where it is consistent with the cosmic neutrino diffuse background flux, $E_\nu^2 \Phi_{\nu_e+\nu_\mu+\nu_\tau} \approx 10^{-8}$ GeV cm^{-2} sec^{-1}sr^{-1}. Because a neutrino telescope looks for $\sim 2\pi$ sky, the parameter space of $N_{\Delta\Omega}^{\rm M} \gtrsim 10^{-6}$ is accessible by a 1 km^3 neutrino telescope with 5 year observation. Null detection of the neutrino multiplets with the criteria of the false alarm rate FAR $\lesssim 0.25$ yr^{-1} leads to the allowed parameter space of

$$\mathcal{E}_\nu^{\rm fl} \lesssim 5 \times 10^{51} \text{ erg}, \quad R_0 \gtrsim 2 \times 10^{-8} \text{ Mpc}^{-3} \text{ yr}^{-1}, \tag{19}$$

PoS(ICRC2023)015

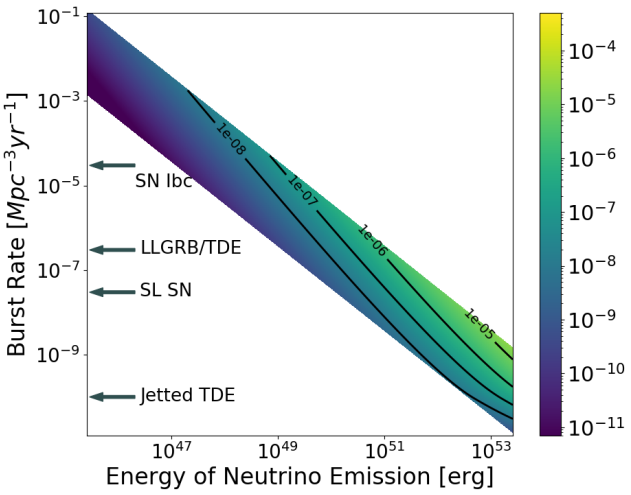

Figure 4: Number of sources to yield neutrino multiplet, $N^{\rm M}_{\Delta\Omega}$, during time $\Delta T = 30$ days in $\Delta\Omega = 1$ deg^2 of sky on the parameter space of $(\mathcal{E}^{\rm fl}_\nu, R_0)$, the output neutrino energy from a source and the burst density rate [27]. A criteria to suppress the annual false alarm rate below ~ 0.25 for 2π sky is applied.

if the transients of $\Delta T \lesssim 30$ days are the major sources to contribute the high energy cosmic neutrino diffuse background radiation [27]. It will constrain the models involving jetted TDEs and super-luminous SNe in future.

4. Summary

The observational fact that the neutrino energy flux at 100 TeV $\sim$ 1 PeV is comparable with that of UHECRs is understandable by the UHECR-neutrino multi-messenger approach. Based upon the framework of photo-hadronic interactions for producing the secondary neutrinos, we have constructed the generic scheme to describe the common sources of UHECRs and high energy neutrinos with less model-dependent way and obtained the viable parameter space required to explain the diffuse high-energy neutrino flux above 100 TeV energies and the UHECR flux above 10 EeV, simultaneously. The five conditions have essentially constrained the allowed parameter space which is rather narrow – requirements for the UHECR acceleration, the UHECR escape, the UHECR nuclei survival, the UHECR energetics, and the fiducial neutrino flux. For an astronomical object with a given photon luminosity, a number density, magnetic field strength, and its equipartition parameter $\xi_{\rm B}$, the basic requirements to qualify as the common sources are represented in the form of conditions of $\xi_{\rm B}$, $p\gamma$ optical depth at UHECR energy of 10 PeV, and the CR loading factor $\xi_{\rm CR}$. Among the known astronomical object classes, we have found that the low luminosity GRBs are the most likely candidate, followed by the jetted TDEs and FSRQs with the extreme parameter tuning. We would like to emphasize, however, that our framework to provide the generic constraints is applicable to as-yet-unknown source populations which may be revealed in future neutrino-driven multi-messenger observations.

PoS(ICRC2023)015

These common source candidates are transients in optical and X-ray bands. In addition, many other neutrino source candidates at TeV sky such as the circumstellar SNe are also transients. Thus it is a key to conduct the multi-messenger follow-up observations in oder to identify the neutrino sources. Overcoming the difficulty that the optical transient sky is filled with numerous SNe, the two approaches have been proposed with the presently operating facilities – introducing a sub-threshold detection channel to a wide field of view X-ray observatory responding to high energy neutrino detection, and the neutrino multiplet detection to trigger ToO observations with optical telescopes. We are living in a new era to utilize neutrino, optical, and X-ray messengers to reveal the origin of cosmic rays, and study the hadronic emissions.

Acknowledgments

The studies written in this article have benefited from the extensive discussions with Kohta Murase. The author is also deeply grateful to Masaomi Tanaka, Nobuhiro Shimizu, and Aya Ishihara for their valuable inputs. Special thanks go to IceCube Collaboration. This work is supported partly by JSPS KAKENHI grant No.18H05206 and 23H04892.

References

[1] Alexander Aab et al. Combined fit of spectrum and composition data as measured by the Pierre Auger Observatory. *JCAP*, 04:038, 2017. [Erratum: JCAP 03, E02 (2018)].

[2] M.G. Aartsen et al. First observation of PeV-energy neutrinos with IceCube. *Phys. Rev. Lett.*, 111:021103, 2013.

[3] M.G. Aartsen et al. Evidence for High-Energy Extraterrestrial Neutrinos at the IceCube Detector. *Science*, 342:1242856, 2013.

[4] M.G. Aartsen et al. Characteristics of the diffuse astrophysical electron and tau neutrino flux with six years of IceCube high energy cascade data. *Phys. Rev. Lett.*, 125(12):121104, 2020.

[5] R. Abbasi et al. Improved Characterization of the Astrophysical Muon–neutrino Flux with 9.5 Years of IceCube Data. *Astrophys. J.*, 928(1):50, 2022.

[6] M. G. Aartsen et al. Detection of a particle shower at the Glashow resonance with IceCube. *Nature*, 591(7849):220–224, 2021.

[7] M.G. Aartsen et al. Differential limit on the extremely-high-energy cosmic neutrino flux in the presence of astrophysical background from nine years of IceCube data. *Phys. Rev. D*, 98(6):062003, 2018.

[8] Shigeru Yoshida and Kohta Murase. Constraining photohadronic scenarios for the unified origin of IceCube neutrinos and ultrahigh-energy cosmic rays. *Phys. Rev. D*, 102(8):083023, 2020.

PoS(ICRC2023)015

[9] Kohta Murase and John F. Beacom. Neutrino Background Flux from Sources of Ultrahigh-Energy Cosmic-Ray Nuclei. *Phys. Rev. D*, 81:123001, 2010.

[10] Shigeru Yoshida and Hajime Takami. Bounds on the origin of extragalactic ultra-high energy cosmic rays from the IceCube neutrino observations. *Phys. Rev. D*, 90(12):123012, 2014.

[11] Kohta Murase and Masataka Fukugita. Energetics of High-Energy Cosmic Radiations. *Phys. Rev. D*, 99(6):063012, 2019.

[12] Kohta Murase, Dafne Guetta, and Markus Ahlers. Hidden Cosmic-Ray Accelerators as an Origin of TeV-PeV Cosmic Neutrinos. *Phys. Rev. Lett.*, 116(7):071101, 2016.

[13] Kohta Murase, Shigeo S. Kimura, and Peter Meszaros. Hidden Cores of Active Galactic Nuclei as the Origin of Medium-Energy Neutrinos: Critical Tests with the MeV Gamma-Ray Connection. *Phys. Rev. Lett.*, 125(1):011101, 2020.

[14] G. Ghisellini, F. Tavecchio, L. Foschini, G. Ghirlanda, L. Maraschi, and A. Celotti. General physical properties of bright Fermi blazars. *MNRAS*, 402(1):497–518, February 2010.

[15] Kohta Murase, Yoshiyuki Inoue, and Charles D. Dermer. Diffuse Neutrino Intensity from the Inner Jets of Active Galactic Nuclei: Impacts of External Photon Fields and the Blazar Sequence. *Phys. Rev. D*, 90(2):023007, 2014.

[16] M.G. Aartsen et al. Constraints on Ultrahigh-Energy Cosmic-Ray Sources from a Search for Neutrinos above 10 PeV with IceCube. *Phys. Rev. Lett.*, 117(24):241101, 2016. [Erratum: Phys.Rev.Lett. 119, 259902 (2017)].

[17] Alexander Aab et al. Probing the origin of ultra-high-energy cosmic rays with neutrinos in the EeV energy range using the Pierre Auger Observatory. *JCAP*, 10:022, 2019.

[18] Shigeo S. Kimura and Kenji Toma. Hadronic High-energy Emission from Magnetically Arrested Disks in Radio Galaxies. *Astrophys. J.*, 905(2):178, 2020.

[19] Daniel Biehl, Denise Boncioli, Cecilia Lunardini, and Walter Winter. Tidally disrupted stars as a possible origin of both cosmic rays and neutrinos at the highest energies. *Sci. Rep.*, 8(1):10828, 2018.

[20] Kohta Murase, Shigeo S. Kimura, B. Theodore Zhang, Foteini Oikonomou, and Maria Petropoulou. High-Energy Neutrino and Gamma-Ray Emission from Tidal Disruption Events. *Astrophys. J.*, 902(2):108, 2020.

[21] Kohta Murase, Kunihito Ioka, Shigehiro Nagataki, and Takashi Nakamura. High Energy Neutrinos and Cosmic-Rays from Low-Luminosity Gamma-Ray Bursts? *Astrophys. J. Lett.*, 651:L5–L8, 2006.

[22] B. Theodore Zhang and Kohta Murase. Ultrahigh-energy cosmic-ray nuclei and neutrinos from engine-driven supernovae. *Phys. Rev. D*, 100(10):103004, 2019.

PoS(ICRC2023)015

[23] Ke Fang, Brian D. Metzger, Indrek Vurm, Elias Aydi, and Laura Chomiuk. High-energy Neutrinos and Gamma Rays from Nonrelativistic Shock-powered Transients. *Astrophys. J.*, 904(1):4, 2020.

[24] Kohta Murase. New Prospects for Detecting High-Energy Neutrinos from Nearby Supernovae. *Phys. Rev. D*, 97(8):081301, 2018.

[25] Kenji Yoshida, Maria Petropoulou, Kohta Murase, and Foteini Oikonomou. Flare Duty Cycle of Gamma-Ray Blazars and Implications for High-energy Neutrino Emission. *Astrophys. J.*, 954(2):194, 2023.

[26] M. Matsuoka et al. The MAXI Mission on the ISS: Science and Instruments for Monitoring All-Sky X-Ray Images. *PASJ*, 61:999, October 2009.

[27] Shigeru Yoshida, Kohta Murase, Masaomi Tanaka, Nobuhiro Shimizu, and Aya Ishihara. Identifying High-energy Neutrino Transients by Neutrino Multiplet-triggered Follow-ups. *Astrophys. J.*, 937(2):108, 2022.

[28] N. Tamura et al. Prime Focus Spectrograph for the Subaru telescope: massively multiplexed optical and near-infrared fiber spectrograph. *Journal of Astronomical Telescopes, Instruments, and Systems*, 1:035001, July 2015.

PoS(ICRC2023)015